



OPEN ACCESS

EDITED BY

Yuedan Wang,
Peking University, China

REVIEWED BY

Lu Xia,
Fudan University, China
Liang Fu,
Shenzhen Third People's Hospital, China

*CORRESPONDENCE

Yayan Niu

✉ yayanniu@163.com

Jianping Zhang

✉ zhangjianping_yb@suda.edu.cn

Peijun Tang

✉ tangpeipei001@163.com

Chunhua Ling

✉ lingchunhua88@126.com

[†]These authors have contributed equally to this work

RECEIVED 04 April 2025

ACCEPTED 26 May 2025

PUBLISHED 18 June 2025

CITATION

Feng Y, Chen Y, Zhang W, Shen X, Yan J, Yao L, Zhang L, Niu Y, Zhang J, Tang P and Ling C (2025) Single-cell analysis of peripheral blood and pleural effusion reveals functional diversity of $\gamma\delta$ T cells in tuberculosis infection. *Front. Immunol.* 16:1605827. doi: 10.3389/fimmu.2025.1605827

COPYRIGHT

© 2025 Feng, Chen, Zhang, Shen, Yan, Yao, Zhang, Niu, Zhang, Tang and Ling. This is an open-access article distributed under the terms of the [Creative Commons Attribution License \(CC BY\)](https://creativecommons.org/licenses/by/4.0/). The use, distribution or reproduction in other forums is permitted, provided the original author(s) and the copyright owner(s) are credited and that the original publication in this journal is cited, in accordance with accepted academic practice. No use, distribution or reproduction is permitted which does not comply with these terms.

Single-cell analysis of peripheral blood and pleural effusion reveals functional diversity of $\gamma\delta$ T cells in tuberculosis infection

Yanjun Feng^{1†}, Yu Chen^{2†}, Wanying Zhang^{1†}, Xinghua Shen¹, Jinyu Yan¹, Lin Yao¹, Lijuan Zhang¹, Yayan Niu^{1*}, Jianping Zhang^{1*}, Peijun Tang^{1*} and Chunhua Ling^{1*}

¹Department of Pulmonary and Critical Care Medicine, The First Affiliated Hospital/Department of Tuberculosis, The Fifth People's Hospital of Suzhou & The Affiliated Infectious Diseases Hospital, Suzhou Medical College of Soochow University, Suzhou, China, ²Department of Biochemistry and Molecular Biology, School of Biology and Basic Medical Sciences, Suzhou Medical College of Soochow University, Suzhou, China

Introduction: Tuberculosis is a contagious airborne disease caused by the *Mycobacterium tuberculosis* infection. $\gamma\delta$ T cells are closely associated with TB infection; however, the specific role of $\gamma\delta$ T cells in the immune response to TB remains unclear, as does the differentiation and mechanism of $\gamma\delta$ T cell subsets in TB patients.

Methods: We analyzed the characteristics of $\gamma\delta$ T subsets in the peripheral blood (Peripheral Blood Mononuclear Cells, PBMC) and pleural effusions (Tuberculous pleural effusion, TPE) and pleural effusions of TB patients using single-cell sequencing to explore the distribution and characteristics of different $\gamma\delta$ T subpopulations.

Results: Seven $\gamma\delta$ T cell subpopulations were identified. The highest percentage of effector $\gamma\delta 2$ cell cluster (C1) was found in PBMCs from TPE patients, accounting for 36.1%, while the highest percentage of tissue-resident $\gamma\delta 2$ cell cluster (C0) was found in PFMCs, reaching 70.5%. Through in-depth analysis, we identified a group of V $\delta 2$ cells exhibiting strong effector function and high expression of *FCGR3A*.

Discussion: Therefore, exploring the mechanism of interaction between V $\delta 2$ cells and *Mtb*, as well as understanding host immune regulation during *Mtb* infection, can not only enhance the understanding of the immune mechanism underlying TB but also provide new theoretical ideas. This research may offer novel therapeutic targets for TB and innovative strategies for treatment and prevention.

KEYWORDS

tuberculosis, *Mycobacterium tuberculosis*, $\gamma\delta$ T cells, *FCGR3a*, single-cell analysis

1 Introduction

Tuberculosis (TB), a disease caused by the *Mycobacterium tuberculosis* complex (MTBC), has become one of the world's deadliest infectious diseases and poses a serious challenge to global health (1). The absence of innovative diagnostic tools, novel therapeutics and effective vaccines presents a major challenge for TB prevention and control, underscoring the importance of research into effective treatment modalities. The development of TB vaccines and immunotherapies represents a promising strategy to combat this disease. $\gamma\delta$ T cells are a unique subsets of T cells with intrinsic immune functions, characterized by their T cell receptor (TCR), which consists of γ and δ chains. Based on the expression of the δ chain of the TCR on the surface of $\gamma\delta$ T cells, these cells can be classified into three subpopulations: V δ 1 T cells, V δ 2 T cells (also known as V γ 9V δ 2 T cells), and V δ 3 T cells (2). V δ 2 T cells are predominantly found in the peripheral blood, accounting for 50% to 90% of the total $\gamma\delta$ T cell population (3). The TCR $\gamma\delta$ on the surface of V δ 2 T cells mainly adopts the pairing of V γ 9 and V δ 2, and is capable of recognizing and activating phosphorylated antigens and secreting perforin, granzyme, etc. to produce cytotoxicity (4). Activated V δ 2 T cells can function as antigen-presenting cells (5). V δ 2 T cells also play an important role in TB (6). They bind to the TCR-CD3 complex via the *Mycobacterium tuberculosis* phosphoantigen isopentenyl pyrophosphate (IPP), which promotes the production of TNF- α and exerts an anti-tuberculosis effect (7, 8). We conducted single-cell sequencing on peripheral blood and pleural effusion samples from five patients with tuberculous pleurisy (TPE) (9) and analyzed the $\gamma\delta$ T cell subset profiles of TPE patients to identify novel effector V δ 2 T-cell potential marker genes, which may provide new therapeutic targets and strategies for the treatment and prevention of TB.

2 Methods

2.1 Single cell sequencing data download and processing

The single-cell datasets HRA000910 and HRA000363, which contain 13 samples, were downloaded from the National Genomics Data Centre (NGDC) Genome Sequence Archive (GSA). The raw data from each sample were subjected to sequencing library demultiplexed and aligned to the human reference genome GRCh38, followed by quantification of UMI counts using 10x Genomics Cell Ranger (v3.1.0). After cell identification using DropletUtils (v1.6.1), the quantified expression matrix was QC'd using the Seurat package (v5.1.0) for R software (v4.4.1). Cells with less than <15% mitochondrial gene content, together with a total gene count >300 and gene expression level between 500 and 15,000 and expressed in at least three cells were retained.

2.2 $\gamma\delta$ T cell filtering and dimensionality reduction clustering

After quality control, the data were filtered for $\gamma\delta$ T cells based on PTPRC, CD3D, CD3E, TRDV1, and TRDV2 gene expression levels greater than 1 using the subset function. The gene expression data were normalized using the NormalizeData function, which employs the default parameters of the Seurat package, the 2000 genes with the largest variations were selected using the FindVariableFeatures function, the gene expression was normalized using the ScaleData function and finally the data were linearly downscaled by PCA using the RunPCA function. The FindNeighbors function was performed by selecting 1:15 PCs based on the ElbowPlot function, and the FindClusters function was performed with a resolution of 0.6. For visual clustering, the RunUMAP function was used with the same number of PCs to generate the Uniform Manifold Approximation and Projection (UMAP) algorithm.

2.3 Cluster cell type identification

Marker genes for each cluster relative to all other clusters were determined using the FindAllMarkers, employing a Wilcoxon test with a p-value <0.05, Bonferroni correction test with p-adj < 0.05 and a differential expression threshold of 0.25, where selected marker genes were expressed in at least 25% of the target cell subpopulations. Each cluster was determined to specifically express the top 3 genes using the COSG package (v0.9.0). The method for gene marker identification based on cosine-based values. Cluster was labeled by manually matching typical cell marker genes with the algorithmically calculated genes that are characteristic of each cluster.

2.4 Analysis of cell cycle

G1/S and G2/M phase signature genes were analyzed using the CellCycleScoring function to predict the temporal cell cycle phases of $\gamma\delta$ T cell subsets.

2.5 Pseudotime analysis of scRNA-seq

Cell trajectories were analyzed using the monocle package (v2.32.0) for the V δ 1 and V δ 2 cell clusters, respectively. Seurat data were analyzed downstream for differential gene expression using a negative binomial distribution model with the newCellDataSet. Normalization was performed using the estimateSizeFactors and estimateDispersions functions, and feature selection was performed with the differentialGeneTest function to filter out 2000 genes that had a significant impact on cell trajectories. The reduceDimension function was employed to reduce the dimensionality of the data using the DDRTree algorithm, and the orderCells function was used to sort

the cells according to their developmental trajectory. The BEAM function was used to model and analyze the branch point-dependent genes within the cell developmental trajectory to obtain the significance score for each gene.

2.6 Pathway enrichment analysis

Enrichment analyses were performed for each cell cluster using the clusterProfiler package (v4.12.6) and the compareCluster function to select the enrichGO Biological Processes (BP) GO database. P-values were corrected using the Benjamini & Hochberg (BH) method. Additionally, pathway enrichment analysis was performed for each cell cluster using the ReactomePA package (v1.48.0) with the compareCluster function to select the Reactome database.

3 Results

3.1 Patients with TPE single-cell sequencing results in PFMCs are distinct from PBMCs

We obtained fresh mononuclear cells from peripheral blood (PBMC) and pleural fluid (PFMC) of five TPE patients for single-

cell sequencing (9), and used the Seurat R package (10) for quality control and screening of the raw sequencing data for $\gamma\delta$ T cells (TRDC) (Figures 1A, B). Ultimately, 959 $\gamma\delta$ T cells from peripheral blood and 1259 $\gamma\delta$ T cells from pleural fluid were included in the study. The screened $\gamma\delta$ T cells were linearly downsampled using principal component analysis (PCA), and the top 15 principal components were then selected for downsampled clustering based on the fragmentation map (Figures 1C, D). The results of the PCA demonstrated that there is a distinction in the transcriptomic profiles exhibited by PBMCs and Pleural Fluid Mononuclear Cells (PFMCs) in TPE patients.

3.2 Single-cell transcriptomics reveals $\gamma\delta$ T cell atlas between PBMCs and PFMCs from patients with TPE

The unsupervised clustering algorithm yielded a total of 7 $\gamma\delta$ T cell subpopulations ranging from 0 to 6, and the top 10 gene heatmaps for each cluster were as follows (Figure 2A). Using the non-linear clustering UMAP method (11) to visualise the $\gamma\delta$ T cell subpopulations, we classified $\gamma\delta$ T cells into 7 clusters (Figure 2B). Consistent with previous PCA results, UMAP visualization results showed that PBMCs and PFMCs from TPE patients have distinct clusters (Figure 2C). Clusters C1, C4, C5, and C6 had a higher

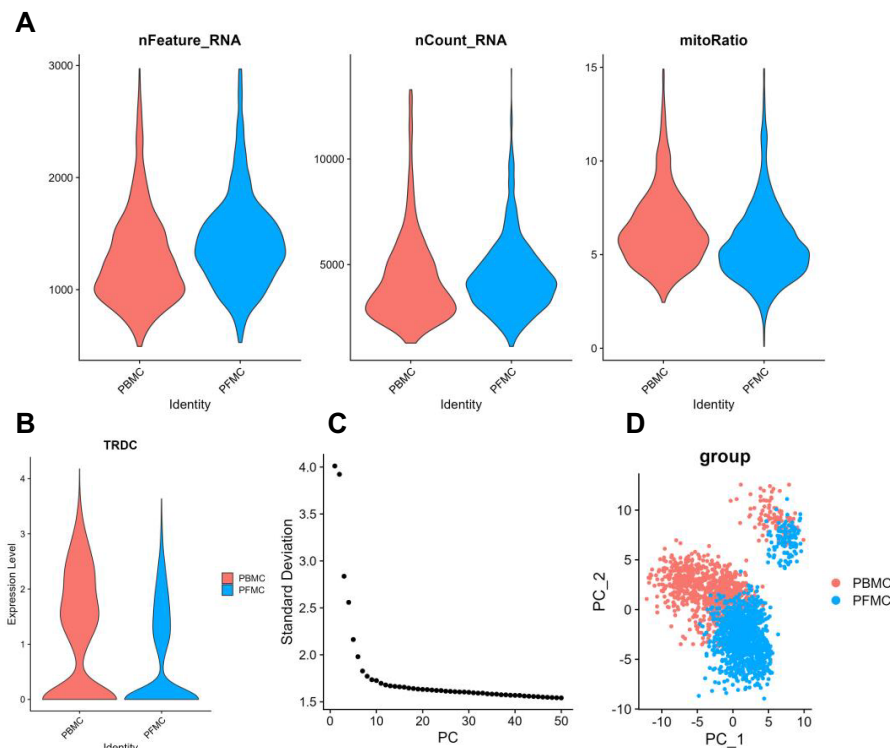
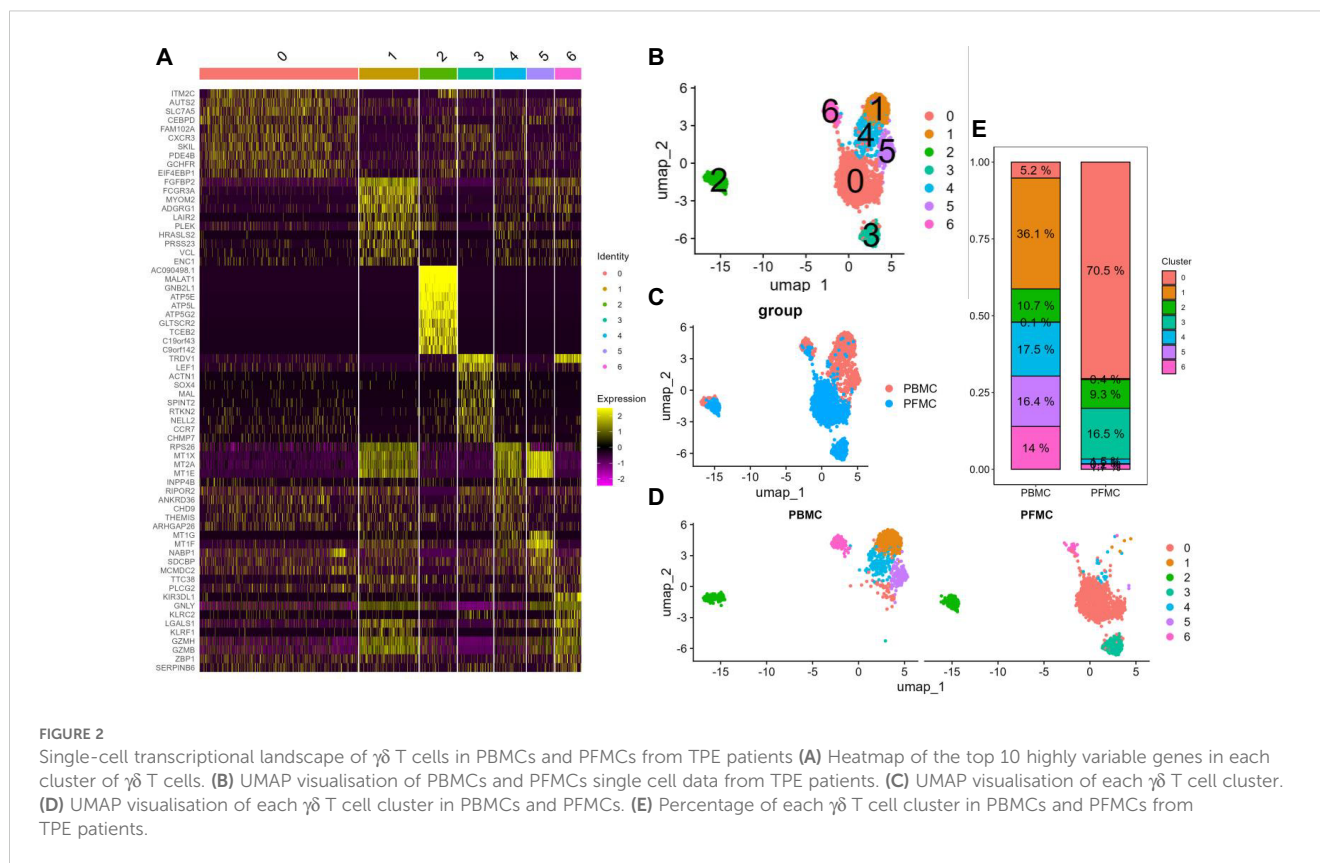


FIGURE 1

Single-cell analysis of PBMCs and PFMCs from TPE patients (A) Violin plots of the number of genes, number of counts and percentage of mitochondrial genes accounted for after quality control of single-cell data in PBMCs and PFMCs from TPE patients. (B) Violin plots of *TRDC* gene expression levels in PBMCs and PFMCs from TPE patients. (C) Principal component fragmentation plots of $\gamma\delta$ T cell single cell data. (D) Visualisation of the principal component analysis of single cell data from PBMCs and PFMCs of TPE patients.



proportion of PBMCs with 36.1%, 17.5%, 16.4%, and 14%, respectively, while PFMCs were more predominant in clusters C0 and C3 with 70.5% and 16.5%, respectively, and cluster C2 is the same in both (Figures 2D, E).

3.3 Heterogeneity of $\gamma\delta$ T cell subsets

According to the expression of $\gamma\delta$ T cell signature molecules (*TRDV1*, *TRDV2*), C3 and C6 were identified as V δ 1 cells, while C0, C1, C2, C4, and C5 were classified as V δ 2 cells (Figure 3A). The scoring calculation of the cell cycle status (12) for each $\gamma\delta$ T cell cluster showed that all seven $\gamma\delta$ T cell subpopulations exhibited the same cell cycle status (Figures 3B, C).

The highest percentage of effector V δ 2 cell cluster (C1) (36.1%), along with elevated expression of cytotoxicity-related genes (*PRF1*, *GZMA*, *GZMB*, *CX3CR1*, and *LAMP1*) and effector transcription factors (*ID2*, *TBX21*, and *ZEB2*) were found in PBMCs from TPE patients. The highest percentage (70.5%) of tissue-resident V δ 2 cell cluster (C0) was found in PFMCs, with high expression of tissue-resident related genes (*ITGAE* and *CD69*) (13), and its high expression of *IL7R* was speculated to be a possible tissue-resident memory V δ 2 cell subpopulation. Central memory V δ 2 cells (C2) was found in both PBMCs and PFMCs, expressing high levels of *CD27*, *IL7R* and mitochondrial oxidative phosphorylation genes (*ATP5E*, *ATP5D*, etc.) (14), as well as cytotoxicity-related genes (*PRF1*, *GZMA*). In PFMCs, there was a higher percentage (16.5%) of naive V δ 1 cell cluster (C3), characterized by elevated expression of

resting stemness-related genes (*TCF7*, *SELL*, *LEF1*, *BACH2*, and *IKZF2*) (15) and almost no expression of effector-related genes. In PBMC, the *INPP4B*⁺ V δ 2 cell cluster (C4) accounted for 17.5% and was characterized by high expression of the inositol phosphatase *INPP4B*, along with elevated expression of metallothionein-related genes (*MT1E* and *MT2A*) (16) (Figures 3D, E). The *MT*⁺ V δ 2 cell cluster (C5) accounted for (16.4%) in PBMCs, which was characterized by high expression of metallothionein-related genes (*MT1E*, *MT2A*, *MT1G*, and *MT1X*) (17, 18). The NK-like V δ 1 cell cluster (C6) accounted for (14%) in PBMCs, which was characterized by high expression of NK-related genes (*GNLY*, *KLRC2*, and *KLRF1*) (19, 20), as well as high expression of cytotoxicity-associated genes (*PRF1*, *GZMA*, *GZMB*, *CX3CR1*, and *LAMP1*) and effector transcription factors (*TBX21* and *ZEB2*) (Figures 3D, E). Taken together, these results reflect the phenotypic and functional heterogeneity of $\gamma\delta$ T cells in PBMCs and PFMCs of TPE patients.

3.4 Trajectory analysis of V δ 2 and V δ 1 T cell subsets among PBMCs and PFMCs

We analyzed the differentiation trajectories of V δ 2 cell subpopulations using pseudotime analysis (21) and found that the tissue-resident V δ 2 cell cluster (C0) was predominantly located in the lower left branch, whereas the effector V δ 2 cell cluster (C1) and the central memory V δ 2 cell cluster (C2) were located in the upper left and right branches, respectively (Figures 4A–C). Based on pseudotime calculations, it was speculated that the tissue-resident

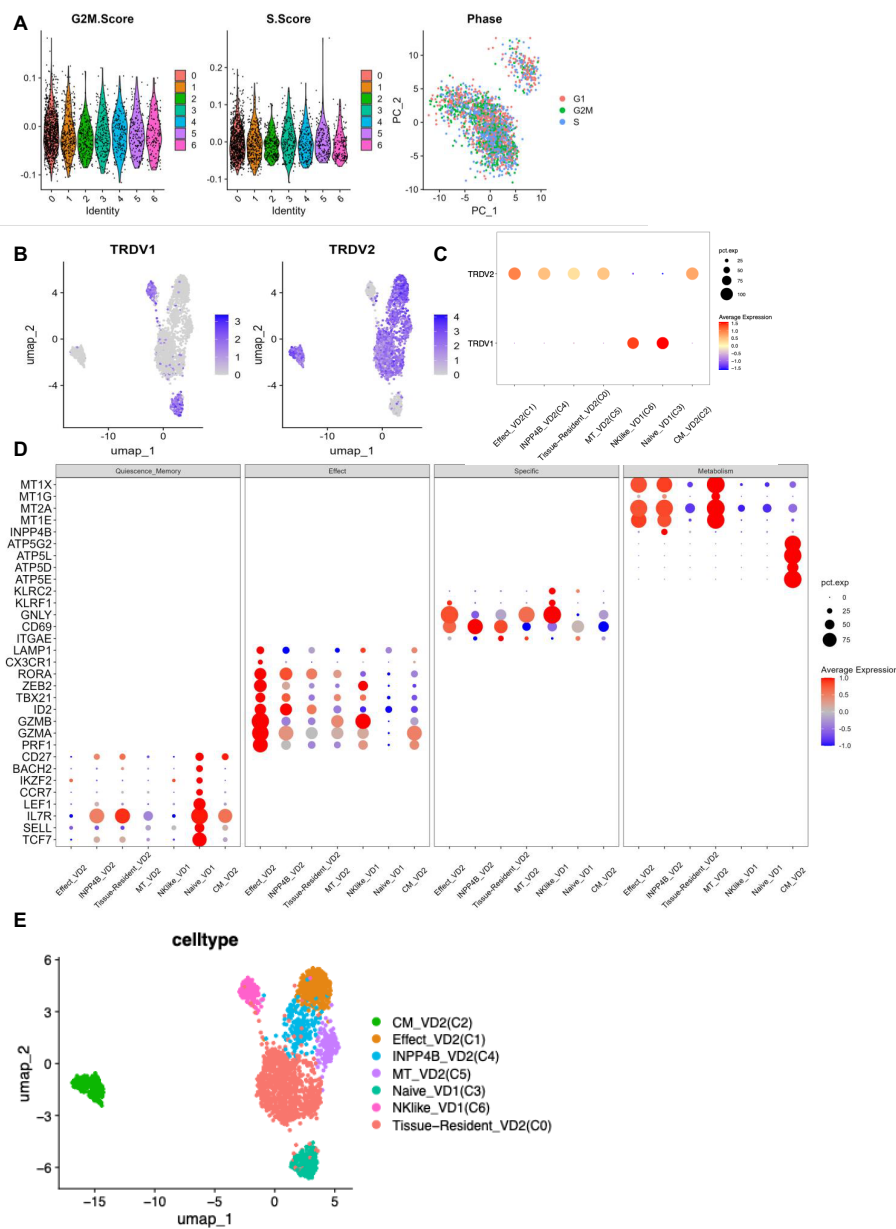


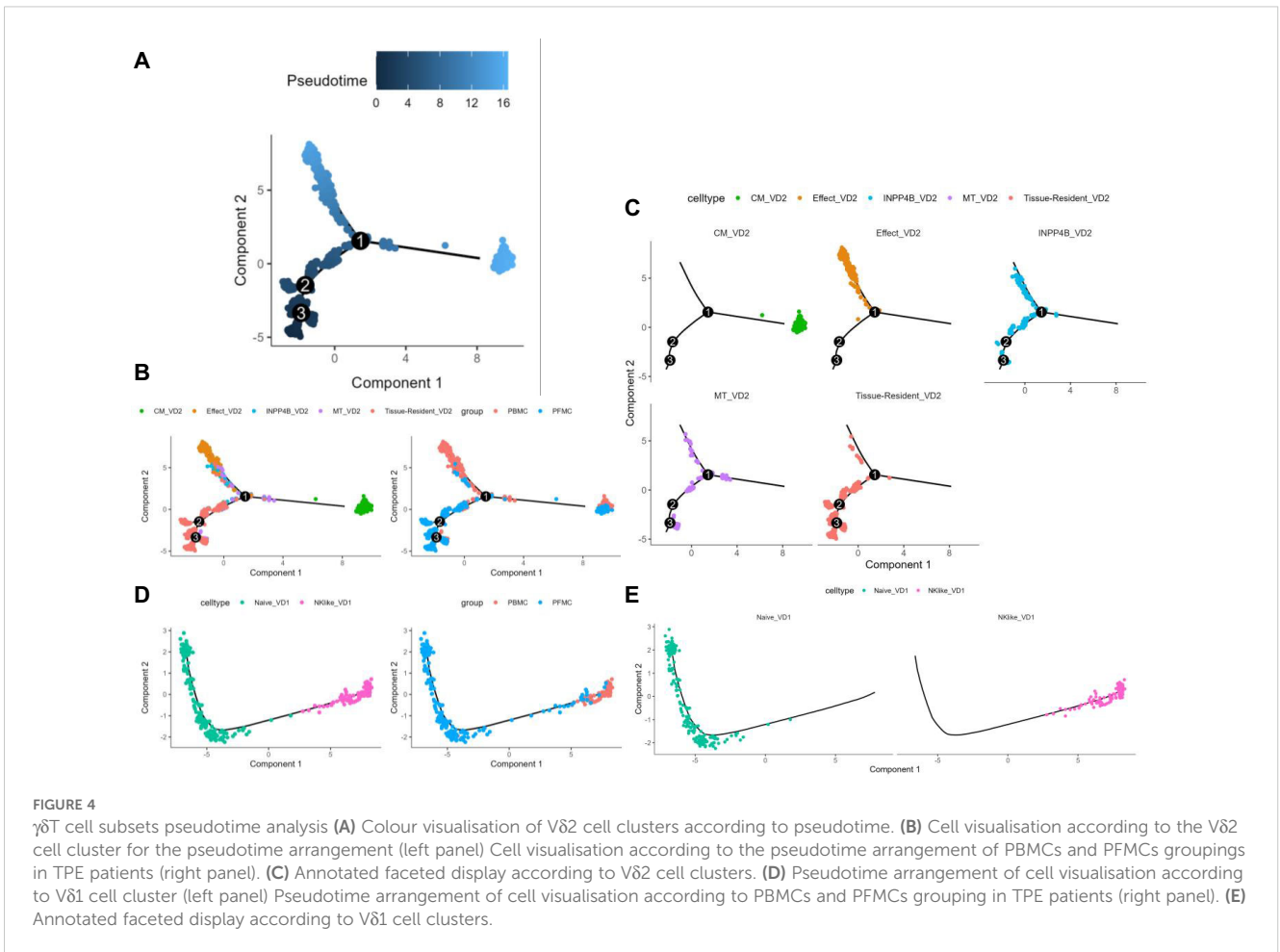
FIGURE 3 $\gamma\delta$ T cell clusters annotation (A) G2M phase scoring violin plot for each cluster of $\gamma\delta$ T cells (left panel) S phase scoring violin plot (middle panel) Visualisation of cell cycle principal component analysis (right panel). (B) *TRDV1* expression in each cluster of $\gamma\delta$ T cells (left panel) *TRDV2* expression in each cluster of $\gamma\delta$ T cells (right panel). (C) *TRDV1* and *TRDV2* expression dot plots in each cluster of $\gamma\delta$ T cells. (D) Expression dot plots of some signature molecules in different clusters of $\gamma\delta$ T cells. (E) UMAP visualisation of $\gamma\delta$ T cell clusters after annotation.

V δ 2 cell cluster (C0) mainly differentiated into the effector V δ 2 cell cluster (C1) and the central memory V δ 2 cell cluster (C2), whereas the INPP4B⁺ V δ 2 cell cluster (C4) and the MT⁺ V δ 2 cell cluster (C5) were mainly located in the intermediate transition state (Figures 4A–C). In contrast, the proposed time series analysis of the differentiation trajectory of the V δ 1 cell cluster showed that there was no branching of the differentiation trajectory, and the naive V δ 1 cell cluster (C3) differentiated into the NK-like V δ 1 cell cluster (C6) (Figures 4D, E). We speculate that the V δ 2 cluster *in situ* in the lungs of TPE patients stimulated by TPE infection has two main directions of differentiation, one into the peripheral blood

to differentiate into a V δ 2 cluster with effector functions, and the other to become a central memory V δ 2 cluster to cope with TPE in the long term. Overall, these results reveal the differentiation trajectory of $\gamma\delta$ T cell subsets.

3.5 Characterizing FCGR3A⁺ V δ 2 cells as a novel subset

Effector V δ 2 cells are the mainstay of the TPE immune response, and further study of the functions and characteristic



genes of these effector V δ 2 cells can enhance our understanding of the TPE immune response of $\gamma\delta$ T cells. Enrichment analysis of biological processes in the GO database²² revealed that a cluster of effector V δ 2 cells exhibited high activation and cytotoxic functions (Figure 5A; Supplementary Material 3). Enrichment analysis of the Reactome database²³ revealed that a cluster of effector V δ 2 cells had specific FCGR-activated signaling pathways (Figure 5B; Supplementary Material 3). We further analyzed the characteristic genes of each cluster using the COSG package²⁴, in which the characteristic gene of the effector V δ 2 cell subpopulation was FCGR3A, and the violin plots also showed that FCGR3A was highly expressed in the effector V δ 2 cell subset (Figures 5C, D). The expression of FCGR3A increased with the differentiation of V δ 2 cells and reached the highest level in the effector V δ 2 cell subset, and at the same time, the expression of FCGR3A with the other cytotoxicity-related genes (PRF1, GZMB and GZMH) and effector transcription factors (TBX21 and ZEB2) had similar pseudotime expression patterns (Figure 5E). We used a regression algorithm to search for pseudotime differential genes in the effector V δ 2 cell cluster, and the heatmap showed FCGR3A as a branching-dependent gene in the effector V δ 2 cell subset (q-value < 0.001) (Figure 5F; Supplementary Material 1).

In conclusion, CD16 (encoded by the *FCGR3A* gene) was specifically expressed in a subset of effector V δ 2 cells in the

peripheral blood of TPE patients and correlated with cytotoxic and effector transcription factor expression.

4 Discussion

Activated V δ 2 T cells secrete a variety of cytokines and chemokines (22, 23). In the context of bacterial infections, such as *Mtb*, the immune system employs a range of cytokines and chemokines. Among these are Th1-type cytokines, including γ -interferon- γ (interferon- γ , IFN- γ), tumor necrosis factor- α (TNF- α), and Th17-type cytokines, such as interleukin-17A (IL-17A) (24–26). These cytokines play a crucial role in immune defense. Furthermore, activated V δ 2 T cells have demonstrated significant cytotoxic activity through the death receptor/death receptor ligand (factor-related apoptosis/factor-related apoptosis ligand, Fas/FasL) and granzyme/perforin pathways (27). Furthermore, an examination of other soluble factors produced by V δ 2 T cells revealed a significant correlation between the level of GZMA production and the inhibition of intracellular *Mtb* growth (27). GZMA proteins secreted by activated V δ 2 T cells are internalised within infected cells, ultimately inhibiting intracellular *Mycobacterium* growth, lysing infected macrophages, and limiting the spread of bacterial diffusion. Consequently, understanding of

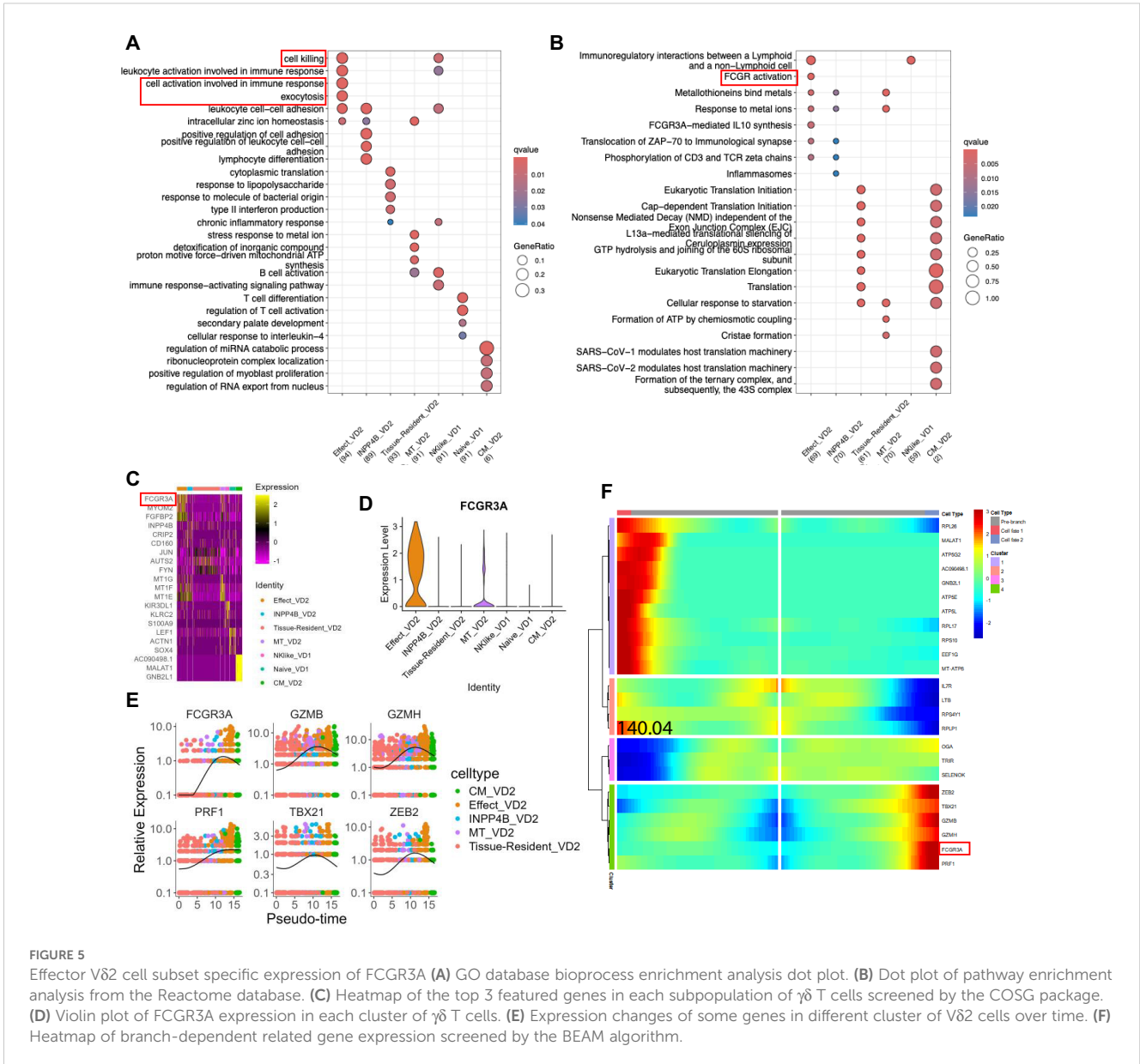


FIGURE 5 Effector Vδ2 cell subset specific expression of FCGR3A (A) GO database bioprocess enrichment analysis dot plot. (B) Dot plot of pathway enrichment analysis from the Reactome database. (C) Heatmap of the top 3 featured genes in each subpopulation of Vδ2 cells screened by the COSG package. (D) Violin plot of FCGR3A expression in each cluster of Vδ T cells. (E) Expression changes of some genes in different cluster of Vδ2 cells over time. (F) Heatmap of branch-dependent related gene expression screened by the BEAM algorithm.

the mechanisms of Vδ2 T cell-Mtb interactions and the host immune regulation during Mtb infection contributes to the development of anti-tuberculosis therapies.

In this study, We re-analyzed the peripheral blood and pleural effusions of TB patients by single cell sequencing and revealed significant phenotypic and functional differences among these subpopulations (9). It was found that Vδ2 T cells predominated in the peripheral blood, especially the effector Vδ2 cell subpopulation (C1), which exhibited high expression of genes associated with cytotoxicity (e.g. *PRF1*, *GZMA*, *GZMB* etc.), and effector transcription factors (e.g., *TBX21*, *ZEB2*), suggesting that these cells possess a potent cell-killing function in the anti-tuberculosis immune response. Conversely, a higher percentage of the tissue-resident Vδ2 cell subpopulation (C0) was identified in pleural effusions, suggesting that these cells may play an important role in the local immune response. Furthermore, the study revealed the naïve state of Vδ1 T cells in pleural effusions (C3) and the NK-

like state in peripheral blood (C6), thus demonstrating the functional diversity of Vδ T cells in distinct tissue environments.

The present study utilized pseudotime analysis to elucidate the differentiation trajectory of Vδ2 T cells. The tissue-resident Vδ2 cell subpopulation (C0) appears to differentiate into two distinct subpopulations: the effector Vδ2 cell subpopulation (C1) and the central memory Vδ2 cell subpopulation (C2). This finding suggests the possibility of distinct differentiation pathways for these cells in response to varying immune demands following TB infection. The higher percentage of the effector Vδ2 cell subpopulation (C1) in peripheral blood suggests that these cells may play an important role in the systemic immune response, whereas the central memory Vδ2 cell subpopulation (C2) may contribute to the formation of long-term immune memory. In addition, the differentiation trajectory of Vδ1 T cells was relatively simple, with the naïve Vδ1 cell subpopulation (C3) differentiating into the NK-like Vδ1 cell subpopulation (C6), suggesting a single pathway of Vδ1 T cell differentiation following TB infection.

A notable finding of this study was the specific expression of CD16 (encoded by the *FCGR3A* gene) in a subpopulation of effector V δ 2 cells. CD16 is an Fc γ receptor commonly associated with the cytotoxic function of natural killer cells (NK cells). The study revealed that *FCGR3A* was expressed at a significantly higher level in a specific subpopulation of effector V δ 2 cells and exhibited a comparable expression pattern to that of genes associated with cell killing (e.g., *PRF1*, *GZMB*, etc.), and effector transcription factors (e.g., *TBX21*, *ZEB2*). This finding suggests that CD16 may play a significant role in the cell-killing function of effector V δ 2 cells. Furthermore, the expression of *FCGR3A* increased with the differentiation of V δ 2 cells, thereby further supporting the critical role of CD16 in effector V δ 2 cell function. This finding provides a new perspective for understanding the mechanism of $\gamma\delta$ T cells in the immune response to TB and may provide potential targets for future immunotherapy.

Despite the findings of the present study, which revealed the functional diversity of $\gamma\delta$ T cells in the immune response to tuberculosis, there are several limitations that must be considered. Firstly, the sample size was relatively small, and larger studies are needed to validate these findings in the future. Secondly, the study primarily focused on the function and differentiation trajectory of $\gamma\delta$ T cells, while the interactions of these cells with other immune cells (e.g., monocytes, dendritic cells, etc.) remain a subject for future investigation. This exploration will contribute to a more comprehensive understanding of the immune response mechanism of TB. Furthermore, the present study is primarily based on transcriptomic data, which can be combined with proteomics and functional experiments in the future research to further validate the function and mechanism of $\gamma\delta$ T cells.

In conclusion, this study revealed the functional diversity and differentiation trajectory of $\gamma\delta$ T cells in tuberculosis patients, especially the critical role of V δ 2 T cells in anti-tuberculosis immunity by single-cell RNA sequencing. The study demonstrated that the effector V δ 2 cell subpopulation exhibit high cytotoxic function, with CD16 (*FCGR3A*) being specifically expressed in this subpopulation, suggesting its role in the immune response to TB. These findings provide novel insights into the mechanisms of $\gamma\delta$ T cells in TB immunity and suggest potential targets for future immunotherapy.

Data availability statement

Publicly available datasets were analyzed in this study. This data can be found here: The single-cell datasets HRA000910 and HRA000363, which contain 13 samples, were downloaded from the National Genomics Data Centre (NGDC) Genome Sequence Archive (GSA).

Ethics statement

Ethical approval was not required for the study involving humans in accordance with the local legislation and institutional

requirements. Written informed consent to participate in this study was not required from the participants or the participants' legal guardians/next of kin in accordance with the national legislation and the institutional requirements.

Author contributions

YF: Conceptualization, Data curation, Formal analysis, Methodology, Writing – original draft. YC: Investigation, Methodology, Writing – original draft. WZ: Data curation, Formal analysis, Methodology, Writing – review & editing. XS: Conceptualization, Data curation, Formal analysis, Writing – review & editing. JY: Conceptualization, Data curation, Formal analysis, Writing – review & editing. LY: Conceptualization, Data curation, Formal analysis, Writing – review & editing. LZ: Conceptualization, Data curation, Formal analysis, Writing – review & editing. YN: Funding acquisition, Methodology, Supervision, Validation, Writing – review & editing. JZ: Funding acquisition, Methodology, Supervision, Validation, Writing – review & editing. PT: Supervision, Validation, Writing – review & editing, Resources. CL: Resources, Supervision, Visualization, Writing – review & editing.

Funding

The author(s) declare that financial support was received for the research and/or publication of this article. This study was supported by grants from Gusu Health Talents Project (GSWS2023063, GSWS2022086, GSWS2022090); Project of Jiangsu Provincial Health Commission (ZD2022041, Ym2023074); Suzhou City health Commission project (LCZX202215, LCZX202216, DZXYJ202309, DZXYJ202411, KJXW2022046); Science and Technology Development Plan of Suzhou Science and Technology Bureau (SKY2022060, SKY2022062, SYW2024013, SKYD2022150, SKYD2023158); National Natural Science Foundation of China (82400008), Respiratory Infectious Diseases Clinical Medical Center of Suzhou, China (Szlcycxz202108).

Acknowledgments

We sincerely thank Professor Xinchun Chen from Shenzhen University School of Medicine for providing the single-cell raw data and permitting its reanalysis, and for helpful discussions on topics related to this work. In addition, we thank the study participants for their contribution.

Conflict of interest

The authors declare that the research was conducted in the absence of any commercial or financial relationships that could be construed as a potential conflict of interest.

Generative AI statement

The author(s) declare that no Generative AI was used in the creation of this manuscript.

Publisher's note

All claims expressed in this article are solely those of the authors and do not necessarily represent those of their affiliated organizations,

or those of the publisher, the editors and the reviewers. Any product that may be evaluated in this article, or claim that may be made by its manufacturer, is not guaranteed or endorsed by the publisher.

Supplementary material

The Supplementary Material for this article can be found online at: <https://www.frontiersin.org/articles/10.3389/fimmu.2025.1605827/full#supplementary-material>

References

1. WHO. *Global tuberculosis report 2024*. Geneva: World Health Organization (2024). Available at: <https://www.who.int/publications/i/item/global-tuberculosis-report-2024>. (Accessed November 25, 2024).
2. Hu Y, Hu Q, Li Y, Lu L, Xiang Z, Yin Z, et al. $\gamma\delta$ T cells: origin and fate, subsets, diseases and immunotherapy. *Signal Transduct Target Ther.* (2023) 8:434. doi: 10.1038/s41392-023-01653-8
3. Jia Z, Ren Z, Ye D, Li J, Xu Y, Liu H, et al. Immune-ageing evaluation of peripheral T and NK lymphocyte subsets in chinese healthy adults. *Phenomics.* (2023) 3:360–74. doi: 10.1007/s43657-023-00106-0
4. Benzaid I, Mönkkönen H, Stresing V, Bonnelye E, Green J, Mönkkönen J, et al. High phosphoantigen levels in bisphosphonate-treated human breast tumors promote $V\gamma 9V\delta 2$ T-cell chemotaxis and cytotoxicity. *In Vivo. Cancer Res.* (2011) 71:4562–72. doi: 10.1158/0008-5472.CAN-10-3862
5. Brandes M, Willmann K, Moser B Professional antigen-presentation function by human gammadelta T Cells. *Science.* (2005) 309:264–8. doi: 10.1126/science.1110267
6. Vorkas CK, Wiperman MF, Li K, Bean J, Bhattarai SK, Adamow M, et al. Mucosal-associated invariant and $\gamma\delta$ T cell subsets respond to initial Mycobacterium tuberculosis infection. *JCI Insight.* (2018) 3:e121899. doi: 10.1172/jci.insight.121899
7. Van Rhijn I, Kasmar A, De Jong A, Gras S, Bhati M, Doorenspleet ME, et al. A conserved human T cell population targets mycobacterial antigens presented by CD1b. *Nat Immunol.* (2013) 14:706–13. doi: 10.1038/ni.2630
8. De Libero G, Singhal A, Lepore M, Mori L Nonclassical T cells and their antigens in tuberculosis. *Cold Spring Harb Perspect Med.* (2014) 4:a018473–a018473. doi: 10.1101/cshperspect.a018473
9. Cai Y, Wang Y, Shi C, Dai Y, Li F, Xu Y, et al. Single-cell immune profiling reveals functional diversity of T cells in tuberculous pleural effusion. *J Exp Med.* (2022) 219:e20211777. doi: 10.1084/jem.20211777
10. Hao Y, Stuart T, Kowalski MH, Choudhary S, Hoffman P, Hartman A, et al. Dictionary learning for integrative, multimodal and scalable single-cell analysis. *Nat Biotechnol.* (2024) 42:293–304. doi: 10.1038/s41587-023-01767-y
11. McInnes L, Healy J, Melville J *UMAP: uniform manifold approximation and projection for dimension reduction.* (2020). doi: 10.48550/arXiv.1802.03426.
12. Nestorowa S, Hamey FK, Pijuan Sala B, Diamanti E, Shepherd M, Laurenti E, et al. A single-cell resolution map of mouse hematopoietic stem and progenitor cell differentiation. *Blood.* (2016) 128:e20–31. doi: 10.1182/blood-2016-05-716480
13. Zakeri N, Hall A, Swadling L, Pallett LJ, Schmidt NM, Diniz MO, et al. Characterisation and induction of tissue-resident gamma delta T-cells to target hepatocellular carcinoma. *Nat Commun.* (2022) 13:1372. doi: 10.1038/s41467-022-29012-1
14. Buck MD, D, Klein Geltink RI, Curtis JD, Chang CH, Sanin DE, et al. Mitochondrial dynamics controls T cell fate through metabolic programming. *Cell.* (2016) 166:63–76. doi: 10.1016/j.cell.2016.05.035
15. Tsui C, Kretschmer L, Rapelius S, Gabriel SS, Chisanga D, Knöpper K, et al. MYB orchestrates T cell exhaustion and response to checkpoint inhibition. *Nature.* (2022) 609:354–60. doi: 10.1038/s41586-022-05105-1
16. Chen ZY, Mortha A INPP4B ensures that ILC1s and NK cells set up a productive home office. *J Exp Med.* (2024) 221:e20232375. doi: 10.1084/jem.20232375
17. Bonaventura P, Benedetti G, Albarède F, Miossec P Zinc and its role in immunity and inflammation. *Autoimmun Rev.* (2015) 14:277–85. doi: 10.1016/j.autrev.2014.11.008
18. Mocchegiani E, Giacconi R, Muti E, Cipriano C, Costarelli L, Tesi S, et al. Zinc-bound metallothioneins and immune plasticity: lessons from very old mice and humans. *Immune Ageing.* (2007) 4:7. doi: 10.1186/1742-4933-4-7
19. Good CR, Aznar MA, Kuramitsu S, Samareh P, Agarwal S, Donahue G, et al. An NK-like CAR T cell transition in CAR T cell dysfunction. *Cell.* (2021) 184:6081–6100.e26. doi: 10.1016/j.cell.2021.11.016
20. Roy Chowdhury R, Valainis JR, Dubey M, von Boehmer L, Sola E, Wilhelmly J, et al. NK-like CD8⁺ $\gamma\delta$ T cells are expanded in persistent Mycobacterium tuberculosis infection. *Sci Immunol.* 8(81):eade3525. doi: 10.1126/sciimmunol.ade3525
21. Qiu X, Mao Q, Tang Y, Wang L, Chawla R, Pliner HA, et al. Reversed graph embedding resolves complex single-cell trajectories. *Nat Methods.* (2017) 14:979–82. doi: 10.1038/nmeth.4402
22. Xu S, Hu E, Cai Y, Xie Z, Luo X, Zhan L, et al. Lysis of a Broad Range of Epithelial Tumour Cells by Human $\gamma\delta$ T Cells: Involvement of NKG2D ligands and T-cell Receptor- versus NKG2D-dependent Recognition. *Scand J Immunol.* (2007) 66:320–8. doi: 10.1111/j.1365-3083.2007.01963.x
23. Milacic M, Beavers D, Conley P, Gong C, Gillespie M, Griss J, et al. DNAX accessory molecule-1 (CD226) promotes human hepatocellular carcinoma cell lysis by $V\gamma 9V\delta 2$ T cells. *Eur J Immunol.* (2009) 39:1361–8. doi: 10.1002/eji.200838409
24. Pereboeva L, Harkins L, Wong S, Lamb LS The safety of allogeneic innate lymphocyte therapy for glioma patients with prior cranial irradiation. *Cancer Immunol Immunother.* (2015) 64:551–62. doi: 10.1007/s00262-015-1662-z
25. Wrobel P, Shojaei H, Schitteck B, Gieseler F, Wollenberg B, Kalthoff H, et al. Stereotoxic administrations of allogeneic human $V\gamma 9V\delta 2$ T cells efficiently control the development of human glioblastoma brain tumors. *Oncol Immunology.* (2016) 5:e1168554. doi: 10.1080/2162402X.2016.1168554
26. Toutirais O, Cabillic F, Le Fric G, Salot S, Loyer P, Le Gallo M, et al. Murine CD27⁽⁻⁾ $V\gamma 6^{(+)}$ $\gamma\delta$ T cells producing IL-17A promote ovarian cancer growth via mobilization of protumor small peritoneal macrophages. *Proc Natl Acad Sci.* (2014) 111:1361–8. doi: 10.1073/pnas.1403424111
27. Pereboeva L, Harkins L, Wong S, Lamb LS Granzyme A produced by $\gamma\delta 2$ T cells induces human macrophages to inhibit growth of an intracellular pathogen. *PLoS Pathog.* (2013) 9:e1003119. doi: 10.1371/journal.ppat.1003119